Combustion and Flame 269 (2024) 113593

Contents lists available at ScienceDirect

Combustion and Flame

journal homepage: www.sciencedirect.com/journal/combustion-and-flame

The influence of heat feedback and thermal conductivity on the burn rate of thermite composites

Keren Shi [1], Yujie Wang [1], George Issac Paul, Michael R. Zachariah [*]

University of California, Riverside, CA 92521, USA

ARTICLE INFO

Keywords:
Heat transfer
Thermal conductivity
Burn rate
Carbon fiber
Thermite

ABSTRACT

In this paper we clarify some concepts related to heat transfer to the reaction front in composite burning. Here, 2.5 wt% carbon fiber (CF) is added to various thermite compositions to assess the effect of thermal conductivity on burn rate. We observe that in some cases the burn rate is enhanced and in others decreased. Upon further analysis we find that this behavior depends on the phase of the reaction product (dispersed vs. continuous). Adding carbon fiber increases the burn rate of composites with a dispersed phase product, which includes Al/MnO_2, Ti/MnO_2 and B/Bi_2O_3. However, CF added to composites with continuous phase product like B/MnO_2, B/Fe_2O_3 and B/Fe_3O_4, the burn rate is reduced. A simple thermal analysis shows that for solid composites with continuous product, increase in thermal conductivity should actually lead to a decrease in burn rate, as any mechanism that bleads energy away for the reaction front will decrease overall reaction velocity. In contrast, for cases where the products are dispersed aerosol droplets, the fibers serve to capture the droplets as they lift off the surface, and thus offers an additional heat feedback mechanism that enhances the burn rate. This study shows that micro-engineering methods to couple heat to the reaction front with minimal loss of heat to the pre-heat zone will result in an increase in power.

1. Introduction

Thermites, typically made from well mixed metals and metal oxides, are a subclass of energetic materials that undergo highly exothermic redox reaction [1]. Compared to the traditional CHNO energetics, thermites have the advantages of higher energy density and higher tunability [2-4]. Despite these advantages, conventional thermites suffer from relatively slow kinetics due to relatively large diffusion length scales between micron scale fuel and oxidizer [3]. Modern formulations utilize nanoscale fuel and oxidizer to increase specific surface area and decrease diffusion length scale for enhanced reactivity [5,6]. Nevertheless, the enhancement in combustion rates is lower than the theoretical prediction and is partially attributed to the loss of nanostructures prior to and during combustion [7-9]. Agglomeration has been commonly observed and studied in energetic composites of different metal fuels [10-15], and various methods have been explored to improve the composite combustion performance by reducing the agglomeration [12,16-20].

Like any self-propagating reacting system, heat feedback, is expected to play a critical role on the reaction velocity [12,19,21-24]. In particular in "pre-mixed systems" heat feedback delivers thermal energy to the reaction front, which serves in some sense as a continuous ignition source for steady propagation. Thus higher levels of heat feedback have been demonstrated to improve burn rate and energy release rate [21-27]. Thermal theories of pre-mixed laminar flame argue that the controlling mechanism of flame propagation is the heat feedback through layers of gas, as heat conducted from reaction zone is necessary to raise temperature of unburned gas to the ignition temperature [27]. From this thinking phenomenological based theories have been derived for the steady-state propagation velocity represented by Eqn. 1, where v is the propagation rate, α is the thermal diffusivity, and $\dot{\omega}$ is the reaction rate [27]. Eqn. 1 suggests that the propagation rate is dependent on how quickly heat is released from the reaction ($\dot{\omega}$) and how quickly heat can be transported to the unburnt region (α).

$$v \sim \sqrt{\alpha \cdot \dot{\omega}} \tag{1}$$

While Eqn. 1 was originally derived for gas phase combustion, research on solid-state systems have concluded similar formulations

* Corresponding author.
E-mail address: mrz@engr.ucr.edu (M.R. Zachariah).
[1] These authors contributed equally.

https://doi.org/10.1016/j.combustflame.2024.113593
Received 8 March 2024; Received in revised form 25 June 2024; Accepted 25 June 2024
Available online 10 August 2024

[28-30]. One of the considerations is how one should manipulate the formulation to enhance the power delivered in the context of Eq. (1). One approach has been applied to manipulate the transport rate (represented by α in Eq. (1)). Embedding materials with high thermal diffusivity into solid propellants for modulating combustion performance has had long history [31]. Caveny et al. first reported significant increases in burn rate of a solid propellant with the addition of metal wires with high thermal diffusivity [28]. Since then, metal wires have been widely utilized to tailor burn rate of solid propellant [32-34].

Recent studies, however, demonstrate an opposite phenomenon: the embedding of materials with low thermal diffusivity improves burn rate of solid energetic composites [31,35,36]. Furthermore, modeling investigations in solid-solid combustion show that a higher thermal diffusivity in a composite lead to a lower burn rate [37,38]. This can be attributed to the concentration of heat generated during the reaction in the adjacent reactants, which allows most of the heat to be utilized to ignite the adjacent reactants rather than being diffused far ahead into the unreacted zone [37]. These studies suggest further consideration of heat transport effects on propagation of composites is warranted.

In this study, carbon fiber was used as an additive to enhance thermal conductivity of nanothermite composites of Al/MnO_2, Ti/MnO_2, B/Bi_2O_3, B/MnO_2, B/Fe_2O_3 and B/Fe_3O_4. The burn rate of these composites was tested by high-speed macroscopic and microscopic imaging. Through the course of this work we found it beneficial to define a new classification for nanothermite composites based on the physical state of the product phase. Composites which generate a "dispersed phase product": are those that produce aerosolized droplets leaving the burning surface. While composites with "continuous phase product" generate solid continuum material during combustion. Adding carbon fiber into composites with a dispersed phase product enhanced the burn rate by trapping particles near the burning interface thus providing more heat feedback to the unburnt sample. However, carbon fiber also showed a negative effect in composites with continuous phase product which was attributed to the increased thermal conductivity in the unreacted region. This presumably led to more rapid energy loss to the unburnt sample and resulted in reduced burn rate. In this paper we explain this behavior in the context of heat-feedback.

2. Experimental section

2.1. Materials

Aluminum nanoparticles (Al, 100 nm, 92 wt% active), titanium nanoparticles (Ti, 30–50 nm, 75 wt% active), boron nanoparticles (B, 100 nm, 85 wt% active), manganese dioxide nanoparticles (MnO_2, 50 nm) and bismuth oxide nanoparticles (Bi_2O_3, 80 nm) were purchased from US research nanomaterials. Iron (III) oxide nanoparticles (Fe_2O_3, <50 nm) and iron (II, III) oxide nanoparticles (Fe_3O_4, <50 nm) were obtained from Sigma-Aldrich. Carbon fiber (CF) was purchased from Composite Envisions (diameter: 7 μm, length: 3 mm). METHOCEL™ F4M hydroxypropyl methylcellulose (HPMC) and Poly(vinylidene fluoride) (PVDF) were purchased from Dow Chemical Co. and Sigma-Aldrich, respectively. N,N-Dimethylformamide (DMF, 99.8 %) was obtained from Fisher Scientific. The active contents of metal nanoparticles were determined by thermogravimetric analysis (STA 449 F3 Jupiter, NETZCSH). All materials were used as received.

2.2. High loading ink preparation and sample fabrication

Al/MnO_2, Ti/MnO_2, B/Bi_2O_3, B/MnO_2, B/Fe_2O_3 and B/Fe_3O_4 nanothermite samples and samples with CF were tested in 90 wt% loading nanocomposites fabricated by direct writing process [39]. The direct writing inks were prepared by first dissolving 50 mg PVDF and 75 mg HPMC into 4 mL DMF. Then a total of 1125 mg of fuel and oxidizer nanoparticles were added into the solution (Table S1). The fuel and oxidizer were at stoichiometric ratio ($\Phi = 1$) determined by the following equation (Eqn. 2–7).

$$4Al + 3MnO_2 = 2Al_2O_3 + 3Mn \quad (2)$$

$$Ti + MnO_2 = TiO_2 + Mn \quad (3)$$

$$B + Bi_2O_3 = B_2O_3 + 2Bi \quad (4)$$

$$4B + 3MnO_2 = 2B_2O_3 + 3Mn \quad (5)$$

$$2B + Fe_2O_3 = B_2O_3 + 2Fe \quad (6)$$

$$8B + 3Fe_3O_4 = 4B_2O_3 + 9Fe \quad (7)$$

For samples with CF, an additional 28 mg (~2.5 wt% of nanothermite) of CF were added into the inks. All inks were sonicated for 30 min after adding each component and magnetically stirred for at least 12 h before printing.

The direct writing processes were performed on Hyrel 30 M printer. The inks were transferred to a 10 mL syringe with an 18-gauge needle and printed on a heated glass plate (~75 °C). 15 layers of ink were printed, and samples were dried at ~75 °C for 30 min after printing followed by 12 h drying at ambient temperature to remove solvent. The printed samples were cut into ~20 mm free-standing sticks for combustion experiments.

2.3. Experiment setup

The samples were taped on the mount inside the testing chamber (Fig. S1). The samples were ignited on the other end by a resistive heated nichrome wire. All samples were tested in argon environment except B/Fe_3O_4 and B/Fe_3O_4/CF samples that were tested in air.

2.4. High speed color camera imaging and burn rate calculation

Macroscopic imaging (Miro M110, Vision Research, resolution ~35 μm per pixel) was used to record the combustion process of all nanothermite samples with and without CF. Microscopic imaging (VEO710L, Vision Research, coupled with Infinity Photo-Optical Model K2 DistaMax, resolution ~1.7 μm per pixel) were performed on samples with dispersed phase product. The exposure time and frame rate were adjusted for each sample individually to ensure that the maximum light intensity was within the detector limit.

The burn rate of each sample was calculated from dividing the burn distance by the burn time from the macroscopic imaging video. Only the center of the samples (~15 mm in length) were used for these calculations to eliminate edge effects.

2.5. Nanocomposites characterization

The cross-sections of the printed nanocomposites were characterized by scanning electron microscope (SEM, Thermo-Fisher scientific NNS450). The porosity of samples was calculated from the sample density (ρ_{sample}) and theoretical density ($\rho_{theoretical}$) by Eqn. 8.

$$porosity = 1 - \frac{\rho_{sample}}{\rho_{theoretical}} \quad (8)$$

3. Results and discussion

3.1. Classification of nanothermite composites by product phases

In the course of this study it became apparent that to understand and explain the observed effects, a classification of the materials based on the type of product phase was highly useful. In particular we observed that the burn rate of different nanothermite composites showed opposite trends upon carbon fiber addition, and that upon further reflection, realized that this behavior appeared to be highly correlated to the nature

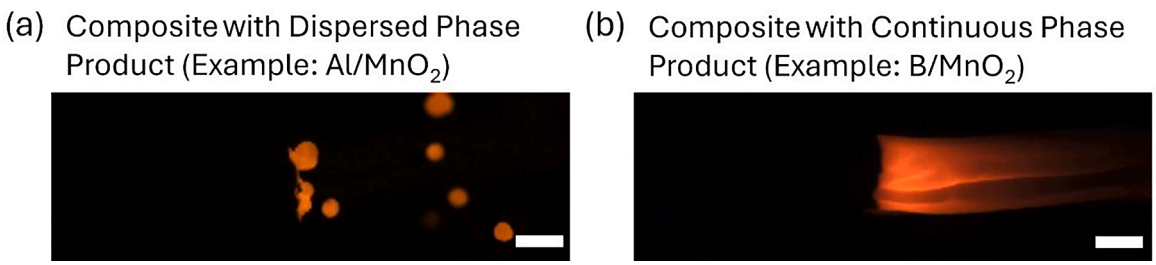

Fig. 1. Examples of the two classes of systems considered (a) combustion of composite with dispersed phase product. (b) combustion of composite with continuous phase product. (scale bar: 1 mm, flames propagate from right to left).

of the product phase. In particular we saw during imaging of propagation, systems with either 1) a dispersed phase (i.e. aerosol) product (Fig. 1a), or 2) a continuous phase (solid-like) product (Fig. 1b).

For composites with dispersed phase product, spherical droplets or fractal-shaped agglomerates form and eject from the burning surface. Typical formulations in this class include Al/MnO_2, Ti/MnO_2, B/Bi_2O_3 and Al/CuO [39]. Adding 2.5 wt% CF into these samples increases the burn rate of the composites. Composites with continuous phase product refers to the composites whose products remain on the unburnt sample (non-aerosol). B/MnO_2, B/Fe_2O_3 and B/Fe_3O_4 composites belong to this class. The addition of 2.5 wt% of CF into these samples has opposite effect as reduced burn rates are observed.

3.2. Carbon fiber enhances the burn rate of composites with dispersed phase product

The combustion of Al/CuO composites with CF has been studied by Wang et al. [39], who observed a ~2.3 × enhancement in burn rate by adding 2.5 wt% CF. Imaging showed that the CF protruding from the burn front intercepted the ejected particles from the burning surface, thus providing more heat feedback to the unburnt sample. To explore the generic nature of this, other chemical formulations were explored in this paper leading to the classification of product phases (dispersed or continuous phase).

Al/CuO nanothermite are composites that can be classified as having a dispersed phased product. Representative images of the combustion of Al/MnO_2 and Al/MnO_2/CF composites are shown in Fig. 2(a) and (d), respectively. Clearly, Al/MnO_2 composites also have dispersed phased products, and the addition of CF serves to intercept the droplets (Fig. 2b and e). Agglomerate residence time on the burning surface is estimated by tracking the time span from the emerging of the agglomerate to the detachment (Fig. S2). The average residence time of the droplets on the burning surface of Al/MnO_2 is found to be ~8 ms (Fig. 2c), while with CF, the average residence time increases significantly to ~26 ms (Fig. 2f). The increased residence time of droplets provides more heat feedback to the unburnt composites and enhances the burn rate. The higher amount of heat feedback results in the burn rate increase from ~41 mm/s to ~57 mm/s (~1.4 × increase) with CF addition.

Other composites with dispersed phase products all showed increased burn rate with CF addition. This includes Ti/MnO_2 and B/Bi_2O_3. Combustion of Ti/MnO_2 composites shows fractal-shaped agglomerates form which are then ejected from the burning surface (Fig. 3a and microscopic image in Fig. S3a). With CF addition, no agglomerate ejection is observed (Fig. 3b and microscopic image in Fig. S3b). Instead, agglomerates attached to the burning surface by the interception of CF. This leads to a longer surface residence time of the agglomerates and a higher amount of conductive heat feedback to the unburnt material, with a ~1.9 × increase in burn rate with CF addition. B/Bi_2O_3 composites also form a dispersed phased product (Fig. 3c and Fig. S3c) with a burn rate of ~9 mm/s. With 2.5 wt% CF additive, the burn rate increases to ~12 mm/s (Fig. 3d and Fig. S3d). The B/Bi_2O_3 composite displays similar combustion characteristics to the Ti/MnO_2 composite despite the smaller size of agglomerates. The addition of CF increases the burn rate ~1.3 × by enhancing heat feedback from the increased agglomerate residence time. This concept has also been applied to a solid propellant where CF has been added into aluminized AP/HTPB propellant, and the burn rate was seen to be enhanced [24].

3.3. Carbon fiber reduces the burn rate of composites with continuous phase product

In contrast to the systems above, here CF addition demonstrates an opposite effect: a decrease in burn rate. These systems all comprise a continuous phase product. Fig. 4a shows that the combustion of B/MnO_2 composites have a continuous phase product with a burn rate of ~10 mm/s (Fig 4a). However, adding CF decrease the burn rate ~0.5 × to ~5 mm/s (Fig. 4b).

More examples with continuous phase product are demonstrated in Fig. 5. The addition of CF to the composites of B/Fe_2O_3 reduces the burn rate from ~7 mm/s to ~6 mm/s, (0.85 × decrease, Fig. 5a and b). For the composite of B/Fe_3O_4, the burn rate decreases ~0.15 ×, from ~7 mm/s to ~1 mm/s with CF addition (Fig. 5c and d). Although all of the nanothermite composites with condensed phase products tested in this study involve boron as the fuel, the B/Bi_2O_3 composites generate dispersed phased product (Fig. 3c), which suggests that phase of the products is also dependent on the oxidizer. The mechanism of the morphology of the product still requires further investigation.

3.4. Proposed mechanism and thermal analysis

We begin our discussion by referring back to a 1-D laminar deflagration, and consider that the temperature profile of nanothermite composites can be divided into three zones by temperature (Fig. 6). First is the pre-heating zone where composites temperature rises from ambient temperature (T_0) to ignition temperature (T_i), and it is assumed that no chemical reaction occurs in this zone. Second is the reaction zone in which temperature increases from T_i to the flame temperature (T_f) and all of the chemical reaction take place in the reaction zone. The product zone follows the reaction zone, and in this zone the product temperature starts to cool down from flame temperature (T_f).

We begin with a simple heat balance. The heat flux balance of the reaction zone can be expressed by Eqn. 9.

$$q_{rxn} = q_r + q_p \tag{9}$$

The heat flux by convection and radiation from flame to burning surface in composites with dispersed phase product are assumed to be small and ignored. Where q_{rxn} is the heat release at the reaction zone and can be expressed in Eqn. 10, where $\dot{Q}_{rxn}$ is the heat release by chemical reaction per unit volume. $v_0 T^n$ represents the heat release rate, where v_0 is the intrinsic burn rate of thermite composites, and T^n accounts for how the intrinsic burn rate changes with preheat temperature. We are assuming CF at such low loadings has no impact on chemistry as previously been shown [39].

$$q_{rxn} = \dot{Q}_{rxn} v_0 T^n \tag{10}$$

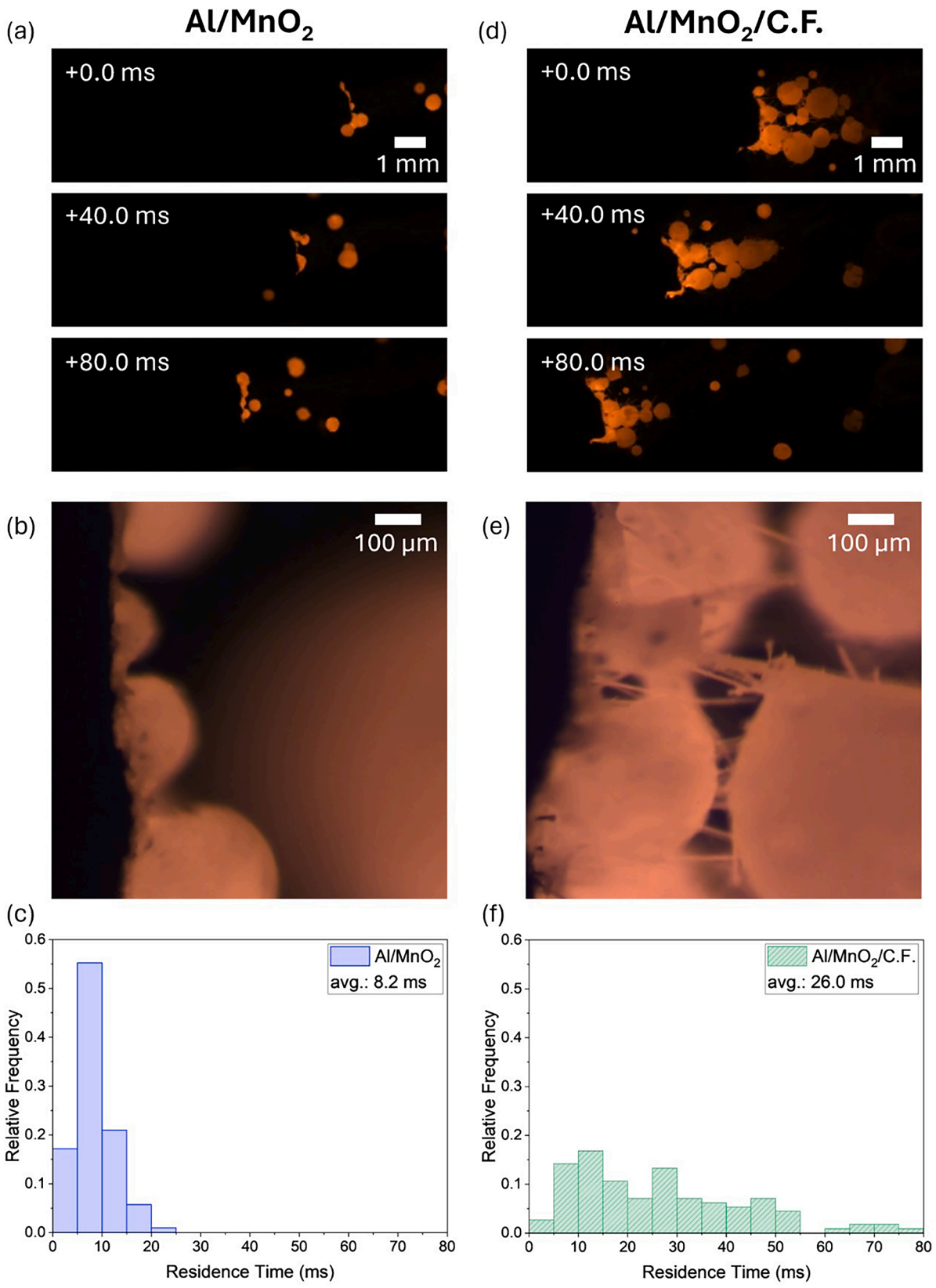

Fig. 2. Combustion of (a) Al/MnO_2 and (c) $Al/MnO_2/CF$ composites (Video S1). Microscopic view of (b) agglomerates ejecting from the burning surface of Al/MnO_2, and (e) agglomerates intercepted by the CF in $Al/MnO_2/CF$ composites. Agglomerate residence time on the burning surface of (c) Al/MnO_2 and (f) $Al/MnO_2/CF$ composites. (flames propagate from right to left).

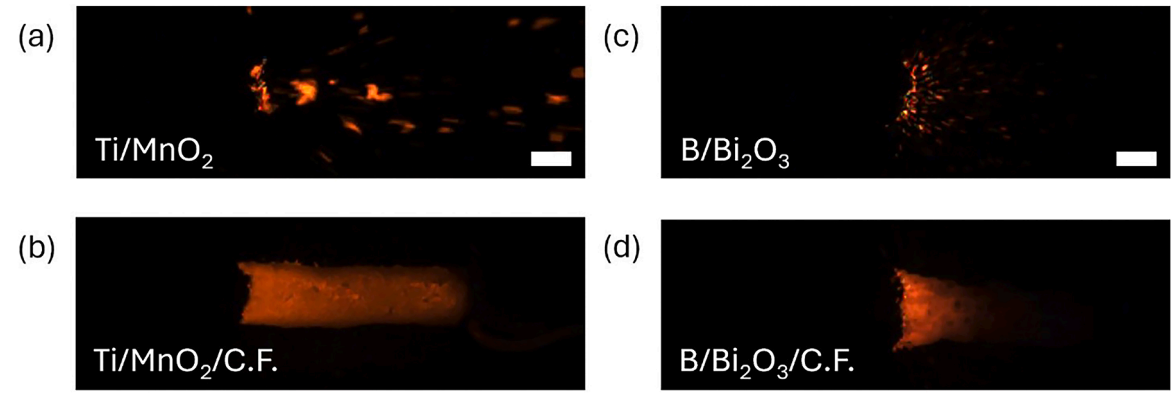

Fig. 3. Combustion of (a) Ti/MnO_2, (b) Ti/MnO_2/CF, (c) B/Bi_2O_3 and (d) B/Bi_2O_3/CF composites. (scale bar: 1 mm, flames propagate from right to left).

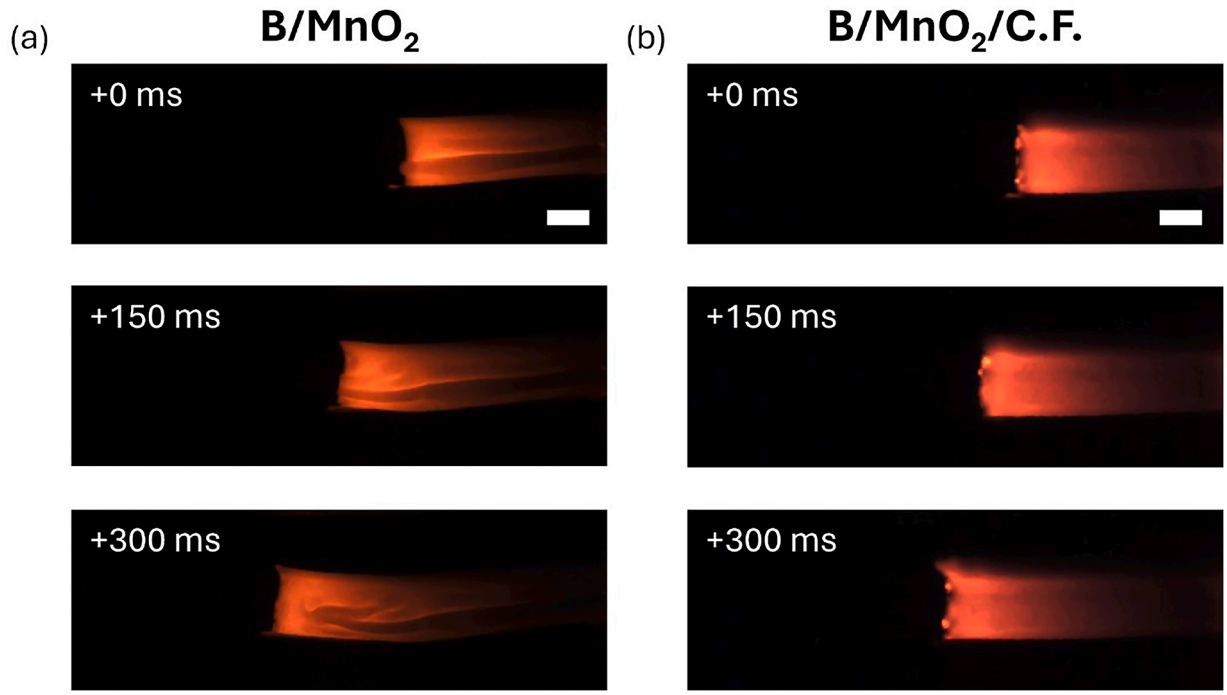

Fig. 4. Combustion of (a) B/MnO_2 and (c) B/MnO_2/CF composites. (scale bar: 1 mm, flames propagate from right to left, video S2).

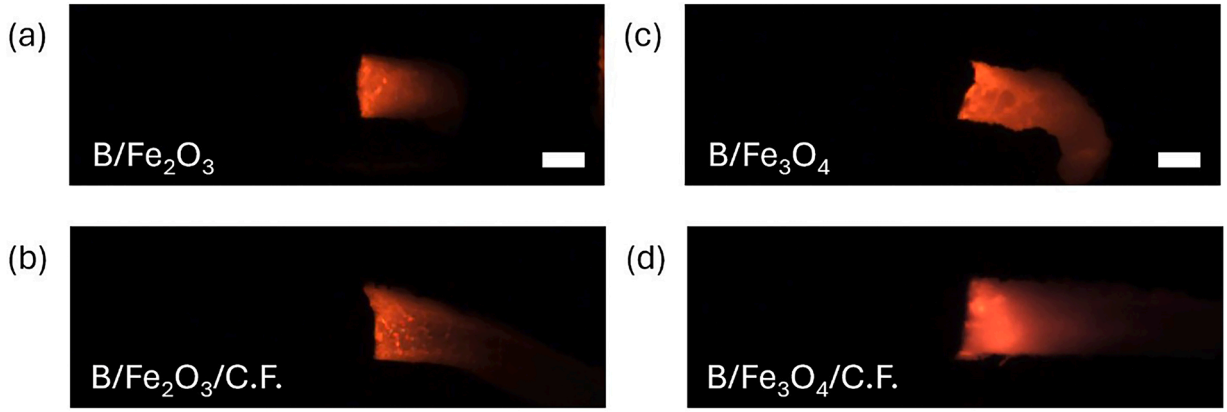

Fig. 5. Combustion of (a) B/Fe_2O_3, (b) B/Fe_2O_3/CF, (c) B/Fe_3O_4 and (d) B/Fe_3O_4/CF composites. (scale bar: 1 mm, flames propagate from right to left).

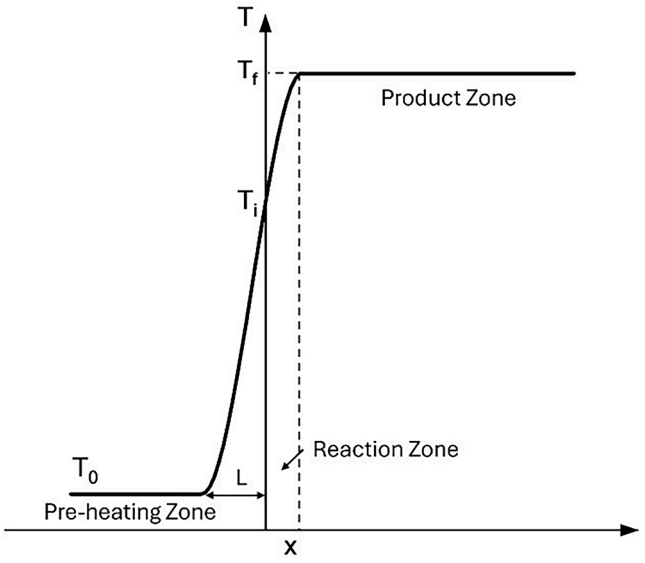

Fig. 6. Temperature profile near the reaction zone of nanothermite composites.

q_p is the heat flux from reaction zone to the product zone represented by Eqn. 11.

$$q_p = u\rho_p c_p T_f \tag{11}$$

Where u *and* ρ_p is the velocity and mass density of the product phase respectively. c_p is the specific heat capacity of the product. At steady-state, mass continuity gives (Eq. (12)).

$$\rho_r v = \rho_p u \tag{12}$$

Where ρ_r is the density of the reactants (composites). Combining Eq. (11) and 12 gives:

$$q_p = v\rho_r c_p T_f \tag{13}$$

q_r represents the heat flux from the reaction zone to the pre-heating zone by conduction. With Eqs. (9), (10), and (13) the burn rate of the nano-thermite composites is:.

$$v = \frac{\dot{Q}_{rxn} v_0 T^n - q_r}{\rho_r c_p T_f} \tag{14}$$

Eq. (14) suggests that an increase in q_r as for example by increasing thermal conductivity of the composite, results in a *decreased burn rate*, assuming other parameters remain constant. In other words any changes to a composite which increases heat loss to the unreacted material actually diminishes the burn rate, assuming chemistry is constant.

These results do not account for any changes in porosity which can play a significant role in influencing the burn rate and a higher porosity leads to an enhanced burn rate [11,40]. However, our measurements in the current study reveal that the addition of CF has minimal effect on the porosity of the composites as listed in Table S2 (SEM images of cross-section of composites in Fig. S4). And adding such a small amount of CF cannot change the chemical reaction between thermites [39]. Therefore, the observed composite burn rate change with CF addition should be closely related to the thermal conductivity increase.

As discussed earlier, according to thermal theories of pre-mixed flames increasing the thermal diffusivity of reaction zone increases the flame propagation rate by facilitating heat transfer rate from the reaction to the unburnt region (see Eq. (1)), while Eq. (14) implies that increasing the thermal diffusivity of the pre-heating zone should decrease the flame velocity. The first thing to note is that application of Eq. (1), is derived assuming that heat flux into the pre-heat zone occurs from the reaction zone so that increasing heat transfer enhances burn. But in the case of composites, where the flame zone and surface are probably indistinguishable **any** transport mechanism that draws heat away from the surface should lower the reaction front temperature, and thus the reaction rate, leading to a decrease in burn rate. This is one way that solid-composites differ from a traditional view of a laminar gas-phase flame.

Adding CF presumably increases the thermal conductivity of the composite and in the context of Eq. (15) should actually decrease the burn rate. And in fact, we do observe this when we have a continuous phase product. A higher thermal conductivity of the composite broadens the thermal wave thickness of the localized pre-heating zone immediately adjacent to the combustion zone, leading to a higher heat loss rate. This results in a reduced burn rate, as illustrated in the right column of Fig. 7. This observation is consistent with the simulation study from Ballas et al. that demonstrates burn rate decreases with increasing thermal conductivity in the unburnt region of a solid-state energetic composite [37]. However, adding CF to the composite with dispersed phase product actually increases the burn rate. This is attributed to the more significant influence of heat feedback on the burn rate, in addition to thermal conductivity of composites. The residence time of the agglomerates on the burning surface is increased by CF which leading to a decrease in q_p. Although, adding CF also increase the thermal conductivity of the composites (q_r term in Eqn. 9), the increased heat feedback outweighs the effect of increased thermal conductivity of the composites, thereby leading to a higher burn rate (left column in Fig. 7). The observed opposite influence of CF to nanothermite composites implies that pre-mixed laminar flame theories cannot be directly applied to the solid-state energetic composite. Future research will focus on obtaining the entire temperature profile during combustion and developing models to quantify the burn rate and thermal property relationship. In principle, the thermal properties of the composites from the reaction zone to the pre-heating zone can be evaluated from the temperature profile and related to the burn rate change in nanothermite composites.

4. Conclusion

In this work, 2.5 wt% carbon fiber is added to various thermite compositions to assess the effect of thermal conductivity on burn rate. We observe that in some cases the burn rate is enhanced and in others decreased. Upon further analysis we find that this behavior depends on the phase of the reaction product (dispersed vs. continuous). Adding carbon fiber increases the burn rate of composites with dispersed phased product including Al/MnO_2, Ti/MnO_2 and B/Bi_2O_3. However, when added to the composites with a continuous phase product like B/MnO_2, B/Fe_2O_3 and B/Fe_3O_4, the burn rate is reduced. A simple thermal theory shows that for solid-composites, an increase in thermal conductivity should actually lead to a decrease in burn rate, as any mechanism that bleads energy away for the reaction front will decrease overall reaction velocity. In contrast for cases where the products are dispersed aerosol droplets, the fibers capture the droplets as they lift off the surface and thus offers an additional heat feedback mechanism that enhances the burn rate. This study shows that micro-engineering methods to couple heat to the reaction front with minimal loss of heat to the pre-heat zone will result in an increase in power.

CRediT authorship contribution statement

Keren Shi: Writing – original draft, Visualization, Formal analysis, Data curation. **Yujie Wang:** Writing – review & editing, Formal analysis, Data curation. **George Issac Paul:** Data curation. **Michael R. Zachariah:** Writing – review & editing, Supervision, Resources, Project administration, Methodology, Investigation, Funding acquisition, Conceptualization.

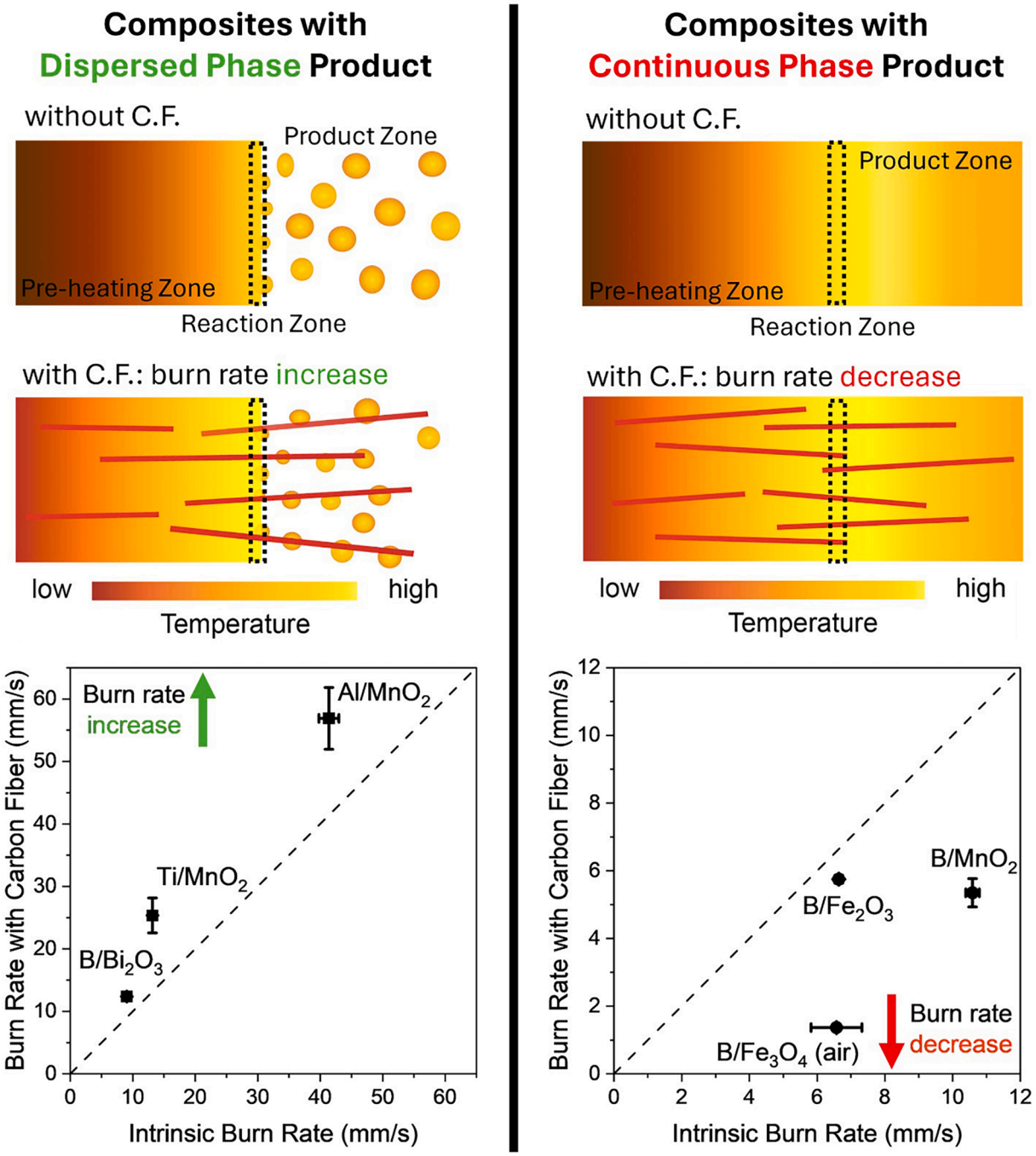

Fig. 7. Conceptual mechanism and examples of CF increasing the burn rate of composites with dispersed phase product (left column). Conceptual mechanism and examples of CF reducing the burn rate of composites with continuous phase product (right column).

Declaration of competing interest

The authors declare that they have no known competing financial interests or personal relationships that could have appeared to influence the work reported in this paper.

Acknowledgments

This work is supported by the AFOSR and ARO.

Supplementary materials

Supplementary material associated with this article can be found, in the online version, at doi:10.1016/j.combustflame.2024.113593.

References

[1] G.C. Egan, K.T. Sullivan, T.Y. Olson, T.Y.-J. Han, M.A. Worsley, M.R. Zachariah, Ignition and combustion characteristics of nanoaluminum with copper oxide nanoparticles of differing oxidation state, J. Phys. Chem. C 120 (2016) 29023–29029.
[2] G. Jian, N.W. Piekiel, M.R. Zachariah, Time-resolved mass spectrometry of nano-Al and nano-Al/CuO thermite under rapid heating: a mechanistic study, J. Phys. Chem. C 116 (2012) 26881–26887.
[3] M.C. Rehwoldt, H. Wang, D.J. Kline, T. Wu, N. Eckman, P. Wang, N.R. Agrawal, M. R. Zachariah, Ignition and combustion analysis of direct write fabricated aluminum/metal oxide/PVDF films, Combust. Flame 211 (2020) 260–269.

[4] Y. Wang, G.I. Paul, E. Hagen, H. Wang, M.R. Zachariah, Combustion behavior of aluminized metal iodate composites. Part 2: iodine and energy release rate, Combust. Flame 262 (2024) 113373.
[5] R.J. Jacob, G. Jian, P.M. Guerieri, M.R. Zachariah, Energy release pathways in nanothermites follow through the condensed state, Combust. Flame 162 (2015) 258–264.
[6] K.T. Sullivan, J.D. Kuntz, A.E. Gash, The role of fuel particle size on flame propagation velocity in thermites with a nanoscale oxidizer, Propellants Explos. Pyrotech. 39 (2014) 407–415.
[7] P. Chakraborty, M.R. Zachariah, Do nanoenergetic particles remain nano-sized during combustion? Combust. Flame 161 (2014) 1408–1416.
[8] K.T. Sullivan, N.W. Piekiel, C. Wu, S. Chowdhury, S.T. Kelly, T.C. Hufnagel, K. Fezzaa, M.R. Zachariah, Reactive sintering: an important component in the combustion of nanocomposite thermites, Combust. Flame 159 (2012) 2–15.
[9] N. Zohari, M.H. Keshavarz, S.A. Seyedsadjadi, The advantages and shortcomings of using nano-sized energetic materials, Cent. Eur. J. Energ. Mater. (2013) 10.
[10] H. Wang, Y. Wang, M.R. Zachariah, Observing coalescence of aluminum nanoparticles during burning using aluminum/ammonia perchlorate sandwiched films, Combust. Flame 260 (2024) 113117.
[11] Y. Wang, E. Hagen, P. Biswas, H. Wang, M.R. Zachariah, Imaging the combustion characteristics of Al, B, and Ti composites, Combust. Flame 252 (2023) 112747.
[12] W. Ao, Z. Fan, L. Liu, Y. An, J. Ren, M. Zhao, P. Liu, L.K.B. Li, Agglomeration and combustion characteristics of solid composite propellants containing aluminum-based alloys, Combust. Flame 220 (2020) 288–297.
[13] C. Tu, X. Chen, Y. Li, B. Zhang, C. Zhou, Experimental study of Al agglomeration on solid propellant burning surface and condensed combustion products, Def. Technol. (2022).
[14] H. Wang, D.J. Kline, M.R. Zachariah, In-operando high-speed microscopy and thermometry of reaction propagation and sintering in a nanocomposite, Nat. Commun. 10 (2019) 3032.
[15] H. Wang, B. Julien, D. Kline, Z. Alibay, M. Rehwoldt, C. Rossi, M. Zachariah, Probing the reaction zone of nanolaminates at ~μs time and ~μm spatial resolution, J. Phys. Chem. C 124 (2020) 13679–13687.
[16] H. Wang, Y. Wang, M. Garg, J.S. Moore, M.R. Zachariah, Unzipping polymers significantly enhance energy flux of aluminized composites, Combust. Flame 244 (2022) 112242.
[17] H. Wang, R.J. Jacob, J.B. DeLisio, M.R. Zachariah, Assembly and encapsulation of aluminum NP's within AP/NC matrix and their reactive properties, Combust. Flame 180 (2017) 175–183.
[18] H. Wang, G. Jian, G.C. Egan, M.R. Zachariah, Assembly and reactive properties of Al/CuO based nanothermite microparticles, Combust. Flame 161 (2014) 2203–2208.
[19] T.R. Sippel, S.F. Son, L.J. Groven, Aluminum agglomeration reduction in a composite propellant using tailored Al/PTFE particles, Combust. Flame 161 (2014) 311–321.
[20] Y. Jiang, H. Wang, J. Baek, D. Ka, A.H. Huynh, Y. Wang, M.R. Zachariah, X. Zheng, Perfluoroalkyl-functionalized graphene oxide as a multifunctional additive for promoting the energetic performance of aluminum, ACS Nano (2022).
[21] D.J. Kline, Z. Alibay, M.C. Rehwoldt, A. Idrogo-Lam, S.G. Hamilton, P. Biswas, F. Xu, M.R. Zachariah, Experimental observation of the heat transfer mechanisms that drive propagation in additively manufactured energetic materials, Combust. Flame 215 (2020) 417–424.
[22] M.Q. Brewster, B.E. Hardt, Influence of metal agglomeration and heat feedback on composite propellant burning rate, J. Propuls. Power 7 (1991) 1076–1078.
[23] H. Wang, D.J. Kline, M.C. Rehwoldt, M.R. Zachariah, Carbon fibers enhance the propagation of high loading nanothermites: in situ observation of microscopic combustion, ACS Appl. Mater. Interfaces (2021).
[24] H. Wang, E. Hagen, K. Shi, S. Herrera, F. Xu, M.R. Zachariah, Carbon fibers as additives to engineer agglomeration and propagation of aluminized propellants, Chem. Eng. J. (2023) 141653.
[25] G.C. Egan, M.R. Zachariah, Commentary on the heat transfer mechanisms controlling propagation in nanothermites, Combust. Flame 162 (2015) 2959–2961.
[26] A. Ishihara, M.Q. Brewster, T.A. Sheridan, H. Krier, The influence of radiative heat feedback on burning rate in aluminized propellants, Combust. Flame 84 (1991) 141–153.
[27] I. Glassman, R.A. Yetter, Combustion, 4th ed, Academic Press, Amsterdam ; Boston, 2008.
[28] L.H. Caveny, R.L. Glick, Influence of embedded metal fibers on solid- propellant burning rate, J. Spacecr. Rockets 4 (1967) 79–85.
[29] A.M. Kanury, A. Hernandez-Guerrero, Steady planar propagation of the gasless SHS reaction producing titanium carbide, Combust. Sci. Technol. 102 (1994) 1–19, 1–6.
[30] A.S. Mukasyan, C.E. Shuck, Kinetics of SHS reactions: a review, Int. J Self-Propag. High-Temp. Synth. 26 (3) (2017) 145–165.
[31] D.J. Kline, M.C. Rehwoldt, H. Wang, N.E. Eckman, M.R. Zachariah, Why does adding a poor thermal conductor increase propagation rate in solid propellants? Appl. Phys. Lett. 115 (2019) 114101.
[32] C. Shuling, L. Fengsheng, Influence of long metal wires on combustion of double-base propellants, Combust. Flame 45 (1982) 213–218.
[33] S. Isert, C.D. Lane, I.E. Gunduz, S.F. Son, Tailoring burning rates using reactive wires in composite solid rocket propellants, Proc. Combust. Inst. 36 (2017) 2283–2290.
[34] N. Kubota, M. Ichida, T. Fujisawa, Combustion processes of propellants with embedded metal wires, AIAA J 20 (1982) 116–121.
[35] S. Shioya, M. Kohga, T. Naya, Burning characteristics of ammonium perchlorate-based composite propellant supplemented with diatomaceous earth, Combust. Flame 161 (2014) 620–630.
[36] H. Wang, J.B. DeLisio, S. Holdren, T. Wu, Y. Yang, J. Hu, M.R. Zachariah, Mesoporous silica spheres incorporated aluminum/poly (vinylidene fluoride) for enhanced burning propellants, Adv. Eng. Mater. 20 (2018) 1700547.
[37] M. Ballas, H. Song, O.J. Ilegbusi, Effect of thermal conductivity on reaction front propagation during combustion synthesis of intermetalics, J. Mater. Sci. 41 (2006) 4169–4177.
[38] H.J. Viljoen, V. Hlavacek, Deflagration and detonation in solid-solid combustion, AIChE J 43 (1997) 3085–3094.
[39] H. Wang, D.J. Kline, M.C. Rehwoldt, M.R. Zachariah, Carbon fibers enhance the propagation of high loading nanothermites: in situ observation of microscopic combustion, ACS Appl. Mater. Interfaces 13 (26) (2021) 30504–30511.
[40] T. Wu, B. Julien, H. Wang, S. Pelloquin, A. Esteve, M.R. Zachariah, C. Rossi, Engineered porosity-induced burn rate enhancement in dense Al/CuO nanothermites, ACS Appl. Energy Mater. 5 (3) (2022) 3189–3198.